■ Subject Heading

Fluorescence-labeled Bis-benzamidines as Fluorogenic DNA Minor-Groove Binders: Photophysics and Binding Dynamics

Jorge Bordello[a], Mateo I. Sánchez[b], M. Eugenio Vázquez[b], José L. Mascareñas[b], Wajih Al-Soufi[a] and Mercedes Novo*[a]

Abstract: During the past decades there has been a great interest in the design of highly sensitive sequence-specific DNA binders. The eligibility of the binder depends on the magnitude of the fluorescence increase upon binding, related to its photophysics, and on its affinity and specificity, which in turn is determined by the dynamics of the binding process. Therefore, the progress in the design of DNA binders requires both thorough photophysical studies and precise determination of the association and the dissociation rate constants involved.

We study two bisbenzamidine (BBA) derivatives labeled through linkers of different length with the dye Oregon Green (OG). These fluorogenic binders show a dramatic fluorescence enhancement upon binding to the minor groove of dsDNA as well as significant improvement in their sequence specificity over the parent bisbenzamidine, although with decreased affinity constants.

The detailed photophysical analysis shows that the static and dynamic quenching of the OG fluorescence by BBA through Photoinduced Electron Transfer (PET) is suppressed upon insertion of BBA into the minor groove of DNA. Fluorescence Correlation Spectroscopy (FCS) yields precise dynamic rate constants that prove that the association process of these fluorogenic binders to dsDNA is very similar to that of BBA alone and that their lower affinity is mainly a consequence of their weaker attachment to the minor groove and the resulting faster dissociation process. The conclusions of this study will allow us to go one step further in the design of new DNA binders with tunable fluorescence and binding properties.

Introduction

Recent years have witnessed an exponential progress on the elucidation of the genetic mechanisms underlying many diseases. As a consequence, there is a renewed interest on the development of synthetic molecules capable of targeting specific DNA sequences, owing to their potential as therapeutic or diagnostic tools. In this context, there have been many reports on the synthesis and biological study of different types of DNA binders,[1, 2] and it has been shown that some of these binders can work as fluorogenic DNA markers.[3] While some of these molecules could be of enormous interest as DNA probes there are very few studies on the interplay between structure, dynamics and photophysical behavior. Moreover, the lack of suitable techniques in addition to experimental hindrances make it difficult to obtain reliable values of the association and the dissociation rate constants of DNA binders. The group of P. Dervan has shown that attachment of specific fluorophores to DNA binding polyamides yields fluorogenic conjugates that display an increase in fluorescence upon interacting with specific DNA sequences. [4-6] Our group has developed alternative, easily accessible, DNA binders based on bis-benzamidine structures, which bind double stranded DNA at specific A/T-rich sites.[7] A major advantage of these molecules derives from their synthetic versatility that allow the straightforward synthesis of derivatives equipped with different functional handles, including fluorescent groups.[8-12] We have recently found that one of these derivatives equipped with Oregon Green (BBA-OG, Figure 1) shows a dramatic fluorescence enhancement upon binding to specific A/T-rich DNA sequences.[13] Additionally, this conjugate displays increased sequence selectivity than its parent bis-benzamidine,[10] although

[a]   Dr. J. Bordello, Prof. Dr. W. Al-Soufi, Prof. Dr. M. Novo
      Department of Physical Chemistry,
      Faculty of Science, Campus Lugo
      University of Santiago de Compostela
      Campus Universitario s/n, 27001 Lugo (Spain)
      Fax: (+982824001)
      E-mail: m.novo@usc.es

[b]   M. I. Sánchez, Prof. Dr. M. E. Vázquez, Prof. Dr. J. L. Mascareñas
      Department of Organic Chemistry
      Faculty of Chemistry and CIQUS, Campus Santiago de Compostela
      University of Santiago de Compostela
      15782 Santiago de Compostela (Spain)

      Supporting information for this article is available on the WWW
      under http://www.chemeurj.org/ or from the author.

with a lower binding affinity, resulting from the presence of the negatively charged fluorophore. Importantly, these binding properties of BBA-OG allowed us to study its DNA binding dynamics by Fluorescence Correlation Spectroscopy (FCS).[14-17] Such single-molecule fluorescence techniques have emerged as powerful tools for the characterization of the kinetics of biosupramolecular interactions[18] and have been successfully applied to the study of DNA-binding with a number of ligands, mainly proteins.[19-21] Our FCS study with BBA-OG demonstrated that its association rate constants are in agreement with those reported for typical minor-groove binders, whereas the dissociation rates are much higher.[22-25] These results suggest that the selectivity of BBA-OG for AT-rich sites mainly arises from the association process, whereas its low affinity constants result from its high dissociation rate constants, which are several orders of magnitude higher than those of the typical minor-groove binders. This increased dissociation could arise from the electrostatic repulsion between the negatively-charged OG fluorophore and the DNA phosphate backbone.
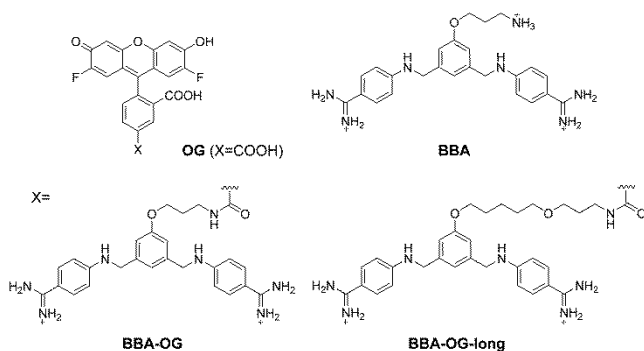
Figure 1. Molecular structures of the compounds used in this work.

In order to better understand the interaction of this binder with DNA, as well as the photophysical mechanisms responsible for the fluorescence enhancement of BBA-OG upon binding, we prepared a new derivative of bisbenzamidine (BBA-OG-long), an analog of the original BBA-OG featuring a longer linker between the bisbenzamidine moiety and the fluorescent marker (see Figure 1). Moving the dye away from the binding moiety is expected to have an effect on the dissociation rates, and consequently on the affinity for different DNA sequences, as well as on the fluorescence properties of the binder.

In this work we present the results of this comparative study, which demonstrate that the fluorescence enhancement upon binding to the DNA arises from the disablement of the Photoinduced Electron Transfer quenching that determines the photophysical properties of the free binders. Furthermore, the FCS study of both dyes indicates that the length of the linker connecting the bisbenzamidine and the fluorophore influences the affinity and specificity of the interaction.

Results and Discussion

Photophysical study of the binders

Oregon Green dyes are fluorinated derivatives of fluorescein with improved properties as fluorescent probes in biological and medical applications, due to their higher photostability and pH-insensitivity under physiological conditions.[26] The fluorescence properties of fluorescein-based probes are mainly due to the xanthene moiety, showing absorption and emission in the visible range and usually very high fluorescence quantum yields.[26, 27] Photoinduced Electron Transfer (PET) has been reported as the mechanism that controls the fluorescence properties of these dyes, so that the substituent-dependent rate of electron transfer from the benzoic acid moiety (electron donor) to the excited xanthene moiety (electron acceptor fluorophore) allows a fine modulation of their brightness and spectral properties.[28, 29] Electron transfer is also responsible for the low quantum yields of some conjugates of fluorescein derivatives with molecules which can act as electron donors that show great potential for biological applications.[30, 31]

Figure 2 shows the excitation and emission spectra of the species used in this study. The minor-groove binder BBA absorbs in the UV range (315 nm) and has a weak emission at about 390 nm. On the contrary, the fluorescence marker OG presents its main absorption and emission bands in the visible range, although it also shows an additional absorption band at 328 nm that overlaps with that of BBA. Linking of these two molecules yields species BBA-OG and BBA-OG-long, which show absorption and emission spectra very similar to those of OG with a slight red shift. Their main emission band appears at 522 nm, independently of the excitation wavelength, although a residual emission is observed in BBA-OG and BBA-OG-long when exciting at 328 nm. Nevertheless, free OG is much brighter than its derivatives. Exciting at 488 nm, OG is 9.0 and 6.5 times brighter than BBA-OG and BBA-OG-long, respectively, as determined by FCS (detection range showed in Figure 2). Additionally, the fluorescence decays of these species are biexponential in contrast to the monoexponential decay of OG (see Table 1). The longest lifetime is similar to that of OG but somewhat smaller and a new shorter lifetime is observed, which makes the main contribution to the fluorescence in the case of BBA-OG.
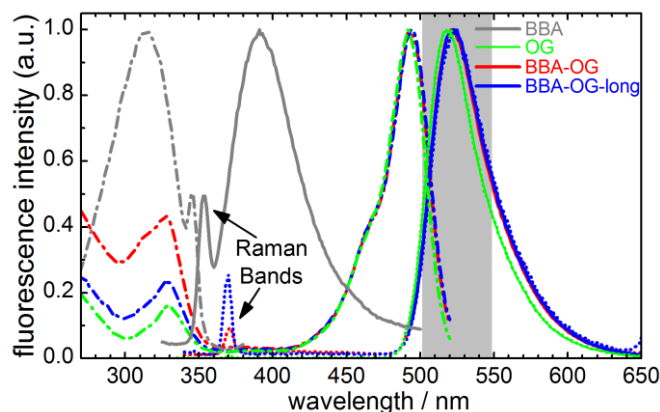
Figure 2. Fluorescence excitation (dashed dotted lines) and emission (solid lines) spectra of BBA (gray), OG (green), BBA-OG (red) and BBA-OG-long (blue). For BBA the spectra were measured at λ_{em}=391 nm and λ_{exc}=315 nm and for OG, BBA-OG and BBA-OG-long, at λ_{em}=525 nm and λ_{exc}=328 nm (dotted lines), 488 nm (solid lines). The spectra were normalized at their maxima to facilitate comparison. The gray area indicates the wavelength range used for FCS measurements.

ChemPubSoc
Europe

DOI: 10.1002/chem.201xxxxxx

CHEMISTRY
A European Journal
Full Paper

Table 1. Fit results of the fluorescence decays of OG and the binders BBA-OG and BBA-OG-long without and with DNA. Fluor2/Fluor3 is the ratio between the contributions to fluorescence of species with lifetime τ_2 and that with lifetime τ_3. τ_1 is a very short lifetime with low contribution arising from experimental artifacts such as Raman light and polarization effects. Emission was monitored at 520 ± 10 nm with excitation at 470 nm.

	τ_1 / ns	τ_2 / ns	τ_3 / ns	FR [e]	χ^2
OG	0.045±0.007		4.156±0.004		1.05
BBA-OG	0.100±0.004	1.55±0.02	3.34±0.07	2.3	1.05
[a]BBA-OG+DNA A/T	0.20±0.03	2.0±0.3	4.30±0.03	0.064	0.98
[b]BBA-OG+DNA G/C	0.144±0.007	1.68±0.04	4.16±0.0	0.61	0.96
BBA-OG-long	0.252±0.004	1.57±0.02	3.99±0.01	0.49	1.08
[c]BBA-OG-long+DNA A/T	0.32±0.01	1.83±0.06	4.26±0.01	0.20	1.08
[d]BBA-OG-long+DNA G/C	0.291±0.006	1.81±0.04	4.17±0.02	0.38	1.05

DNA concentrations: [a] 282 µM; [b] 239 µM; [c] 306 µM; [d] 299 µM.

[e] FR=Fluor2/Fluor3

These results indicate that BBA-OG and BBA-OG-long present similar fluorescence properties as OG, but they undergo a quenching process that leads to a much lower fluorescence quantum yield and a shorter lifetime of the OG moiety. Moreover, the second lifetime observed in these species must be related to the quenching process, since BBA does not absorb/emit under the conditions used in these measurements. When comparing the two derivatives, it is observed that fluorescence quenching is more effective in BBA-OG, where the linker between BBA and OG is shorter. All these facts suggest that the quenching process is due to an interaction between BBA and OG.
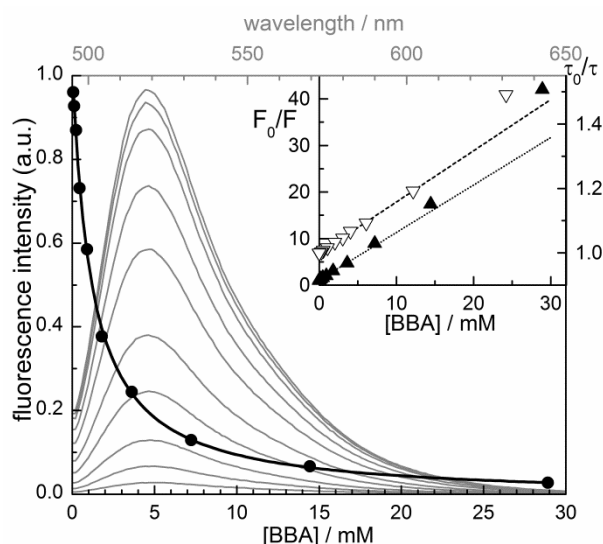
Figure 3. Fluorescence emission spectra of OG in the presence of different concentrations of BBA (thin gray lines) and fluorescence intensity at 520 nm against BBA concentration (black circles) with the fitted curve (thick black line) using the model described in text. Excitation wavelength: 488 nm. Inset: Stern-Volmer plots of fluorescence intensity at 520 nm (black triangles, slope = 1019 ± 24 mol^{-1} dm^3) and of τ_3 (white triangles, slope = 15.9 ± 0.2 mol^{-1} dm^3).

In order to test this hypothesis, the fluorescence emission spectra and the decays of OG in the presence of different concentrations of BBA were measured. A dramatic decrease of the fluorescence intensity with the addition of BBA is observed (Figure 3). Moreover, the corresponding Stern-Volmer plot is clearly non-linear at high BBA concentrations, suggesting that both static and dynamic quenching take place. In fact, the decrease of the longer lifetime (τ_3), associated to OG, as the concentration of BBA is increased (Table 2) evidences collisional quenching. The Stern-Volmer slope obtained for this lifetime is about two orders of magnitude smaller than that determined for the fluorescence intensity at low BBA concentrations (see inset in Figure 3), indicating that the observed decrease of the fluorescence intensity is mainly due to static quenching. Time-resolved measurements yield a second, shorter lifetime at BBA concentrations higher than 2 mM, whose amplitude is small but positive and increases with BBA concentration. This lifetime is attributed to the complex formed between OG and BBA (static quenching), which should have a very low contribution to fluorescence due to its low quantum yield.

Table 2. Fit results of the fluorescence decays of OG in the presence of different concentrations of BBA. Triexponential fits with τ_1=0.08 ± 0.03 ns^{-1}. Fluor2/Fluor3 is the ratio between fluorescence contributions of species with lifetime τ_2 and that with lifetime τ_3. Emission monitored at 520 ± 10 nm with excitation at 470 nm.

[BBA] / mM	τ_2 / ns	τ_3 / ns	FR [a]	χ^2
0		4.156±0.004		1.06
0.293		4.137±0.001		1.19
0.554		4.118±0.001		1.17
1.07		4.084±0.002		1.05
2.05	1.7±0.5	4.019±0.007	0.008	1.11
3.04	2.3±0.7	3.97 ±0.02	0.023	1.12
4.05	1.8±0.6	3.89±0.01	0.012	1.04
6.06	1.7±0.2	3.80±0.01	0.036	1.11
12.1	1.4±0.2	3.48±0.02	0.059	1.00
24.2	1.0±0.1	2.78±0.02	0.11	1.01

[a] FR=Fluor2/Fluor3

$$OG^* + BBA \xrightarrow{k_1} OG{:}BBA^* \xrightarrow{k_E} OG^-{:}BBA^{+\,*}$$

$$h\nu \updownarrow k_{OG} \qquad h\nu \updownarrow k_{OG{:}BBA} \qquad \downarrow \text{no fluor}$$

$$OG + BBA \underset{}{\overset{K_q}{\rightleftharpoons}} OG{:}BBA$$
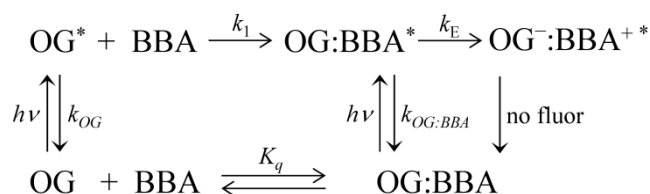
Scheme 1. Mechanism proposed for the photophysical behavior of OG in the presence of BBA including the formation of a complex between OG and BBA in the ground state (K_q, quenching equilibrium constant) and a dynamic quenching in the excited state with rate constant k_1. k_E is the rate constant for the photoinduced electron transfer process which yields a non-fluorescent charge-transfer complex.

On the basis of these results, a mechanism is proposed for the interaction of OG with BBA (Scheme 1) that includes the formation of a complex between OG and BBA in the ground state (K_q, equilibrium constant) and the dynamic quenching of OG by BBA (k_1, bimolecular rate constant) in the excited state. Electrostatic forces between the two molecules with charges of opposite signs favor the formation of an ion-pair complex between BBA and OG moieties, where Photoinduced Electron Transfer (rate constant k_E) would be very effective since the distance between donor (BBA) and acceptor (OG) is very short. This kind of process has been observed for other conjugates of fluorescein derivatives with electron donors.[30, 31] Collisional quenching also takes place, but it is less effective since the two molecules have to diffuse together.

The proposed formation of a complex in the ground state was demonstrated by measuring the absorption spectra of OG in the presence of different concentrations of BBA. Small but systematic changes of the absorption spectrum of OG were observed with the typical pattern of a 1:1 complexation equilibrium (data not shown). In spite of the distortions caused by the tail of the BBA absorption band, estimations were obtained for the complexation equilibrium constant ($K_q = (0.7 \pm 0.3) \times 10^3$ mol^{-1} dm^3) and for the spectra of the two species involved, free OG and complex OG:BBA (see Figure 1S in SI). Under experimental conditions using excess of BBA with respect to OG, the mechanism in Scheme 1 leads to equation (1) for the steady-state fluorescence intensity at a certain emission wavelength λ, $F(\lambda)$, as a function of the total BBA concentration, [BBA]. $F_{OG}(\lambda)$ and $F_{OG:BBA}(\lambda)$ are the fluorescence intensities at the emission wavelength λ of free OG and complex OG:BBA, respectively, and ε_{OG} and $\varepsilon_{OG:BBA}$ are their molar absorptivities at the excitation wavelength.

$$F(\lambda) = F_1(\lambda) + F_2(\lambda)$$

$$F_1(\lambda) = F_{OG}(\lambda) \frac{1}{(1 + K_q[\text{BBA}])(1 + R_1[\text{BBA}])}$$

$$F_2(\lambda) = F_{OG:BBA}(\lambda) \frac{R_\varepsilon R_1[\text{BBA}] + (1 + R_1[\text{BBA}]) K_q[\text{BBA}]}{(1 + K_q[\text{BBA}])(1 + R_1[\text{BBA}])}$$

$$R_\varepsilon = \varepsilon_{OG} / \varepsilon_{OG:BBA}$$

$$R_1 = k_1 / k_{OG}$$

(1)

The resolution of the corresponding differential equations leads to biexponential functions for the fluorescence decays of OG in the presence of different concentrations of BBA, with lifetimes:

$$\tau_A = 1 / (k_{OG} + k_1[\text{BBA}])$$

$$\tau_B = 1 / (k_{OG:BBA} + k_E)$$

(2)

In order to prove the validity of the mechanism and to estimate the rate constants involved, global analysis were performed for the series of fluorescence emission spectra and the series of fluorescence decays, using as fit functions those given in equations (1) and (2), respectively. Analysis of the decays is very satisfactory (see Figure 2S in SI) and yields the rate constants given in Table 3, corresponding to the deactivation of the two species (k_{OG} and the sum $k_{OG:BBA} + k_E$, which cannot be resolved) and the collisional quenching constant k_1, as well as the

preexponential factors, which are related to concentration and quantum yield of those species. The value obtained for k_1 is similar to those reported for other PET intermolecular quenching constants, such as the quenching of coumarins by aromatic amines or by nucleosides.[32, 33] The latter case had many similarities to the system under study, since also static quenching takes place that yields a complex detectable in lifetime measurements.[33]

The information obtained in the analysis of the decays, specifically the ratio $R_1 = k_1 / k_{OG}$, was used for the global fits of the series of fluorescence emission spectra together with the ratio of molar absorptivities $R_\varepsilon = \varepsilon_{OG} / \varepsilon_{OG:BBA}$ estimated from the pure absorption spectra of OG and complex OG:BBA (Figure 1S in SI). As shown in Figure 3 for the data measured at 520 nm, the fits are very satisfactory and yield a value for the equilibrium constant K_q (Table 3) that is of the order of magnitude expected for the formation of such ion pairs[34, 35] and observed for ground-state complexes between polyamides and tetramethylrhodamine.[4] Moreover, the pure emission spectrum estimated for the complex OG:BBA in these analyses (Figure 3S in SI) is slightly red-shifted with respect to that of free OG and shows a two orders of magnitude lower intensity. The low fluorescence quantum yield of this complex is similar to those of other fluorescein derivatives where PET is very efficient.[28, 29]

Table 3. Values of the equilibrium constant K_q and the rate constants involved in the mechanisms proposed for the interaction between OG and BBA (Scheme 1) and for the binders BBA-OG and BBA-OG-long (Scheme 2). The errors given are the uncertainties of the fits for two series of experimental data.

Parameter	OG + BBA	BBA-OG	BBA-OG-long
K_q, K_q' /10^3	(0.83 ± 0.02) mol^{-1} dm^3	0.36	0.09
k_{OG} /10^9 s^{-1}	0.2408 ± 0.0001	0.23	0.23
$(k_{OG:BBA} + k_E)$ /10^9 s^{-1}	0.64 ± 0.08	0.64 ± 0.01	0.64 ± 0.01
k_1, k_1' /10^9 s^{-1}	(3.7 ± 0.2) mol^{-1} dm^3	0.07	0.02
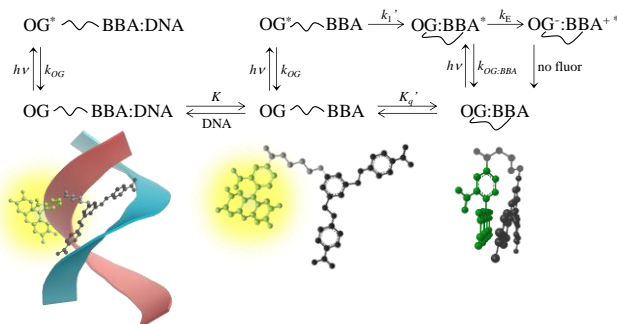
Scheme 2. Mechanism proposed for the photophysical behavior of the binders BBA-OG and BBA-OG-long, including the formation of an intramolecular complex in the ground state (K_q', quenching equilibrium constant) and the dynamic quenching in the excited state with a unimolecular rate constant k_1'. k_E is the rate constant for the photoinduced electron transfer process which yields a non-fluorescent charge-transfer complex. In the presence of DNA there is a competitive ground-state equilibrium (K, binding equilibrium constant) which yields a complex between the BBA moiety of the binders and DNA with the typical fluorescence of OG. A sketch of the open and closed conformations of the binders and of the complex with DNA is shown at the bottom.

On the basis of these results, a similar mechanism can be proposed to explain the photophysical behavior of the binders BBA-OG and BBA-OG-long (Scheme 2), which includes static quenching due to the formation of a ground-state intramolecular complex (K_q', equilibrium constant) and dynamic quenching in the uncomplexed molecules with an unimolecular rate constant k_1'. Since the electron donor and the acceptor are linked by flexible chains, the two processes are expected to be more effective than with the free molecules but differences should be observed between the two binders of different linker lengths.

According to the proposed mechanism (Scheme 2), the lifetime τ_2 of the binders (Table 1) corresponds to complex OG:BBA, yielding deactivation rates ($k_{OG:BBA} + k_E$) that coincide for the two binders and also for the complex formed between the free species (Table 3). Lifetime τ_3 is attributed to the unfolded molecules where BBA and OG are too far away to form a complex in the ground state, so that it corresponds to the deactivation rate of free OG, which is affected by the excited-state dynamic quenching with rate constant k_1'. The values of k_1' for the two binders are then obtained from the relation: $\tau_3 = 1/(k_{OG} + k_1')$ and using a value for the deactivation rate of the OG moiety slightly lower than that of free OG, taken from the results obtained in the presence of DNA (Table 1). (Note that, as shown in Figure 1, the substituents in the benzoic moiety are different for the free OG used in this work (carboxylic acid) and for the binders (amide group) and they control the fluorescence properties by modulating the rate of intramolecular photoinduced electron transfer from the benzoic moiety to the xanthene.[28, 29]) As expected for the great dependency of the electron-transfer rate on the distance between donor and acceptor,[32] the value of k_1' is significantly higher in BBA-OG than in BBA-OG-long, indicating that the shorter linker facilitates the formation of encounter complexes appropriate for a successful PET reaction.

For the estimation of the ground-state equilibrium constant K_q', we used the fluorescence ratio between the species with lifetimes τ_2 and τ_3 obtained in the time-resolved measurements (Fluor2/Fluor3 in Table 3). This ratio is given by the following equation, which can be easily derived from equation (1) replacing the products k_1 [BBA] and K_q [BBA] by k_1' and K_q', respectively:

$$\frac{\text{Fluor2}}{\text{Fluor3}} = \frac{F_{OG:BBA}(\lambda)}{F_{OG}(\lambda)} \left(\frac{\varepsilon_{OG}}{\varepsilon_{OG:BBA}} \frac{k_1'}{k_{OG}} + K_q' + K_q' \frac{k_1'}{k_{OG}} \right) \qquad (3)$$

In this equation the ratio $F_{OG:BBA}(\lambda)/F_{OG}(\lambda)$ for the measuring wavelength (520 nm) is estimated as 0.005 ± 0.001 from the time-resolved fluorescence titrations of OG with BBA (Table 2) and the ratio $\varepsilon_{OG:BBA}/\varepsilon_{OG}$ for the excitation wavelength (470 nm) is obtained from the pure absorption spectra of free OG and complex OG:BBA (Figure 1S in SI). With this information and the values of k_1' determined before, the equilibrium constant K_q' can be calculated for the two binders (Table 3). The value obtained for BBA-OG is 4 times higher than that of BBA-OG-long, indicating again that the shorter linker favors the formation of a complex between the two moieties. From the values of K_q' we can estimate the equilibrium concentrations, resulting in 99.7% and 98.9% of ground-state complexes for BBA-OG and BBA-OG-long, respectively. This difference leads to the estimation that the binder with the shorter linker is approximately 2 times brighter than that with the longer linker, in quite good agreement with the values obtained in FCS measurements.

It is interesting to compare the results obtained for our binders with those reported for other conjugates undergoing PET between the two linked moieties. The intramolecular quenching rate constants k_1' are of the same order of magnitude as those determined for conjugates of Coumarin 120 with different nucleoside phophorothionates and show similar ratios with the corresponding intermolecular rate constants (k_1).[33] Static quenching was also observed for these systems, and in some cases the fluorescence lifetime of the complex could be detected, although our binders show much higher ground-state equilibrium constants probably due to electrostatic interactions between the charged moieties. There are also some examples of conjugates where a fluorescein derivative is linked to an electron donor, yielding molecules of much lower quantum yields with improved properties as fluorescent probes.[30, 31] Finally, fluorescence static quenching was observed for DNA binders formed by polyamides linked to tetramethylrhodamine, which was attributed to PET processes.[4]

Photophysics of the binders in the presence of DNA

Once the photophysical behavior of the binders under study is understood, we analyze the changes in their fluorescence properties due to interaction with DNA. Figure 4 shows the fluorescence excitation and emission spectra of BBA-OG and BBA-OG-long under conditions of selective excitation/emission of the OG moiety in the absence and in the presence of DNA with A/T and G/C sequences.
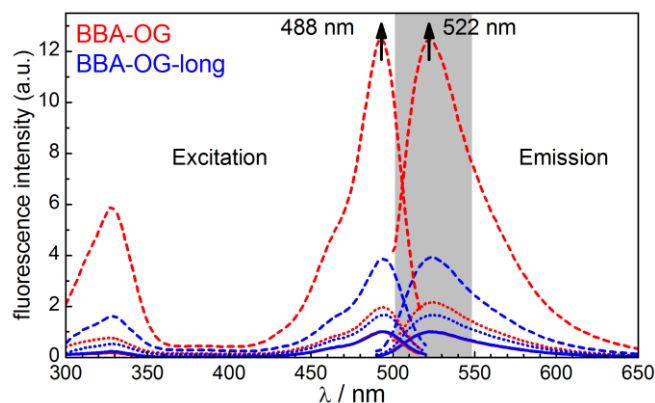
Figure 4. Fluorescence excitation and emission spectra of BBA-OG (red) and BBA-OG-long (blue) without (solid lines) and with DNA AAATTT-hp (dashed lines) and GGCCC-hp (dotted lines) at the same DNA concentrations as given in Table 1. The excitation spectra were obtained at 522 nm emission and the emission spectra were monitored at 488 nm excitation. The spectra of the two binders without DNA were normalized at their maxima to facilitate comparison. The grey area indicates the wavelength range used for FCS measurements.

As discussed before, the emission spectra obtained by excitation of the OG moiety of BBA-OG or BBA-OG-long are very similar to that of OG (Figure 1), but show a significant decrease of intensity resulting from the static and dynamic quenching of OG by the BBA moiety. Addition of DNA causes an increase of the fluorescence intensity without spectral change, which is more pronounced for AT-rich sequences than for GC-rich sequences (Figure 4). This must be due to the interaction of the binding BBA

moiety with DNA to form complexes DNA:BBA-OG, which prevents both static and dynamic quenching of the OG moiety. As proposed in Scheme 2, the complexation with DNA competes with the formation of the low-fluorescent intramolecular complexes OG:BBA,. Also dynamic quenching cannot take place when the BBA moiety is bound to DNA. Consequently, DNA:BBA-OG complexes will show similar fluorescence properties as free OG. A similar effect has been observed for DNA binders formed by polyamides and tetramethylrhodamine.[4]

For both binders the fluorescence increase is larger for A/T than for G/C sequences (Figure 4). This must be attributed to the higher affinity of these minor-groove binders for A/T-rich DNA rather than to the different fluorescence properties of the complex formed with DNA, as has been recently reported for BBA-OG.[13] Furthermore, BBA-OG shows much larger fluorescence increase than BBA-OG-long upon complexation with DNA as it could be expected for the higher quenching efficiency observed in the binder with the shorter linker. The also possible differences in the binding constants of BBA-OG-long to DNA will be analyzed below.

The results of the lifetime measurements (Table 1) are in agreement with the mechanism proposed in Scheme 2. Lifetime τ_2 of the binders, which was attributed to complex OG:BBA, is also observed after addition of DNA but its contribution to fluorescence decreases significantly due to the lower concentration of this complex. The observed lifetime τ_3 is a mean value of the lifetimes of the OG moiety in free and bound unfolded binders, weighted by the relative contributions to fluorescence of these species. In the case of A/T sequences, the value of τ_3 increases in the presence of DNA approaching a limiting value of about 4.3 ns attributed to the lifetime of the bound unfolded binder in the complex DNA:BBA-OG, which does not show dynamic quenching. For the low affinity G/C sequences this limiting value is not observed at similar DNA concentrations because of the higher contribution of the free unfolded binder molecules with shorter lifetime. As for the fluorescence intensity, these effects are larger for BBA-OG in comparison to BBA-OG-long due to the higher efficiency of quenching in this binder with a shorter linker.

Binding dynamics

The fluorescence changes of a dye upon binding to a host make it possible to determine the corresponding association and dissociation rate constants from FCS curves, providing that the binding dynamics is faster than diffusion.[14-17] Then FCS titrations allow also for the determination of the binding equilibrium constant K and other properties of the binder. This is the case for BBA-OG when binding to DNA, as already reported,[13] and also for the analogue BBA-OG-long, as shown below.

First we compare the FCS curves of BBA-OG and BBA-OG-long in the absence of DNA (thin solid lines in Figure 5). Both curves show similar diffusion terms whose correlation times correspond to the translational diffusion times of the free binders (τ_f). Also similar bunching terms are observed that must be attributed to triplet formation with correlation times that correspond to their triplet lifetimes (τ_T). The individual fits of equation (5) without reaction term to these FCS curves are very satisfactory and yield the characteristic parameters of the free binders (Table 4). The translational diffusion coefficients can be

easily obtained from the experimental diffusion correlation times using the relation $D = w_{xy}^2 / 4\tau_D$ for a calibrated detection volume, and are in agreement with those calculated from their molar masses assuming a conformation of spherical particles ($D \sim M^{-1/3}$), as found for other similar molecules.[36] The two binders have very close diffusion coefficients, as expected for their comparable molar masses. Analysis of the FCS curves obtained in power series for the two binders confirmed that the bunching term is due to triplet formation and yielded precise values for τ_T (Table 4). Both triplet lifetime and triplet amplitude are similar for the two binders.
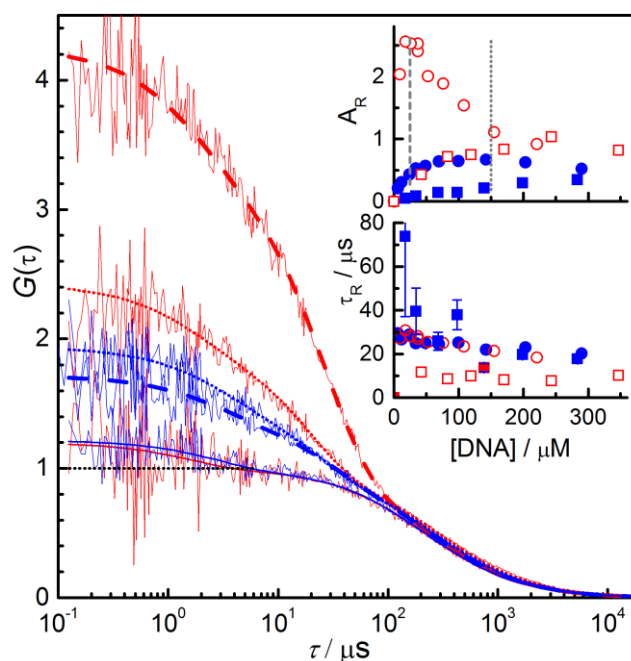
Figure 5. Experimental and fitted fluorescence correlation curves of BBA-OG (red lines) and BBA-OG-long (blue lines) in the absence of DNA (thin solid lines) and in the presence of different concentrations of AAATTT-hp DNA: 26.0 µM (red dashed lines), 23.9 µM (blue dashed lines), 155 µM (red dotted lines) and 142 µM (blue dotted lines). Insets: variation of the relaxation amplitude A_R and the relaxation time τ_R with $[DNA]_0$ obtained from the individual fits of equation (5) to the experimental data of FCS titrations (see Figures 4S and 5S in the SI) for BBA-OG with AAATTT-hp (red open circles), BBA-OG with GGCCC-hp (red open squares), BBA-OG-long with AAATTT-hp (blue closed circles) and BBA-OG-long with GGCCC-hp (blue closed squares). The two vertical lines at 25 µM (dashed) and 150 µM (dotted) indicate approximately the DNA concentrations of the correlation curves represented in the main panel. Parameters w_{xy}/w_z and τ_T were fixed at the values determined in calibration measurements and in power series, respectively.

Table 4. Characteristic values of the binders BBA-OG and BBA-OG-long free and bound to DNA in aqueous solution obtained in the fits of the FCS curves: translational diffusion coefficients of free (D_f) and bound (D_b) binder, triplet lifetime (τ_T) and amplitude of the triplet term (A_T) at the irradiance used for FCS titrations.

System	$D_f / 10^{-10}$ m^{2}s^{-1}	$D_b / 10^{-10}$ m^{2}s^{-1}	τ_T / µs	A_T
BBA-OG	3.2	1.2	2.2	0.20
BBA-OG-long	3.1	1.2	2.7	0.21

CHEMISTRY
A European Journal
Full Paper

DOI: 10.1002/chem.201xxxxxx

ChemPubSoc
Europe

Addition of DNA causes significant changes in the FCS curves of both binders (Figure 5), basically a shift of the diffusion term to longer correlation times and the appearance of a second bunching term. This new term must be attributed to the binding reaction dynamics (G_R in equation (5)) and is characterized by a reaction correlation time τ_R and an amplitude A_R. As previously reported,[13] the amplitude of the reaction term is exceptionally high in the case of BBA-OG in the presence of A/T DNA. This is due to the huge brightness ratio q between bound and free dye that contributes quadratically to A_R, as given in equation (8). For BBA-OG-long much lower amplitudes are observed since the increase of fluorescence intensity upon binding is smaller, as discussed above (see Figure 4). The shift of the diffusion term is due to the binding process that leads to a complex binder:DNA of much higher molar mass than the free binder and therefore longer diffusion time (see Scheme 2).

FCS titrations were performed for each binder with A/T and G/C DNA (see reference [13] for titrations of BBA-OG and Figures 4S and 5S for titrations of BBA-OG-long). Individual fits of each FCS curve to equation (5) yield, among other parameters, the values of amplitude A_R and correlation time τ_R of the reaction term that are plotted against DNA concentration in Figure 5. The concentration dependencies of τ_R and A_R are those expected for these parameters and described by equations (7) and (8), respectively. The reaction time decreases as the concentration of DNA is increased, varying in the range 40 - 10 μs approximately, so that it can be well separated from the triplet term. The reaction amplitude increases first with DNA concentration and then decreases again, showing a maximum that depends on the magnitude of the binding constant K and the brightness ratio q. Note that for BBA-OG with A/T DNA the maximum of A_R arises at a low DNA concentration and this allows for the determination of the binding parameters (equilibrium constant and association/dissociation rate constants) at very low extents of the binding reaction. This is a result of the high brightness ratio q of this binder that is very convenient for the use of FCS to determine binding dynamics.[17]

Analysis of the mean diffusion time, the reaction time, and the reaction amplitude obtained in the individual fits as functions of DNA concentration using equations (6), (7) and (8) yield estimates of the binding equilibrium constant K and the rate constants k_+ and k_-. Nevertheless, more precise values can be obtained by global "target" analysis using as dataset the whole series of FCS curves obtained in a titration and equation (5) as fit function with the parameters $\bar{\tau}_D$, τ_R and A_R substituted by their model functions, given by equations (6), (7) and (8), respectively. The term global refers to the fact that some fit parameters are shared among all curves: the diffusion times of free (τ_f) and bound binder (τ_b), the dissociation rate constant (k_-), the equilibrium constant (K) and the brightness ratio between bound and free binder (q). The association rate constant (k_+) is not fitted directly but obtained from the fitted values of k_- and K. In order to avoid parameter correlation, the diffusion time of the free binder (τ_f) is fixed to the experimental value obtained in the absence of DNA and the diffusion time of the binder bound to DNA (τ_b) is fixed to the value obtained from the diffusion coefficients of the complexes estimated on the basis of reported experimental data.[37] The relaxation time of the triplet (τ_T) and its amplitude (A_T)

are considered to be independent of $[DNA]_0$ since no significant differences in the triplet term were observed in power series measured for the binders in the presence of DNA. Therefore these two parameters are also shared and τ_T is fixed to the value obtained for the free binder (Table 4). The mean number of particles in the sample volume (N) and the baseline were set as individual fit parameters for each curve.

Table 5. Binding equilibrium constant (K), association (k_+) and dissociation (k_-) rate constants, and brightness ratio (q) of BBA-OG and BBA-OG-long with DNA-hp of two sequences: AAATTT and GGCCC. These results were obtained by global "target" fit of each series of FCS curves measured by titration of the binders with DNA as described in text.

System	$K/10^3 M^{-1}$	$k_+/10^8 M^{-1}s^{-1}$	$k_-/10^4 s^{-1}$	q
BBA-OG+AAATTT	4.27±0.03	1.36±0.01	3.19±0.02	12.4±0.1
BBA-OG+GGCCC	0.059±0.001	0.083±0.003	14.0±0.4	10.9±0.1
BBA-OG-long+AAATTT	3.6±0.1	1.33±0.04	3.7±0.1	4.2±0.1
BBA-OG-long+ GGCCC	0.28±0.04	0.13±0.02	4.7±0.3	4.0±0.2

The good quality of the global fits can be observed in Figures 4S and 5S for the titrations of BBA-OG-long (see reference [13] for the titrations of BBA-OG). The fitted curves are in very good agreement with the experimental ones and the residuals show random distribution. The results obtained for the fit parameters related to the binding process are given in Table 5. Figure 6 shows a logarithmic plot of the rate constants obtained for the two binders in order to facilitate their comparison. A first look to the results shows that the parameter most affected by the linker length of the binders is the brightness ratio q. The values obtained reveal a 3-fold higher fluorescence enhancement upon binding to DNA for BBA-OG, reflecting the above-discussed larger efficiency of the quenching process in this binder due to the shorter linker. In the case of BBA-OG there is a small effect of the DNA sequence on q that may be due to structural differences between the two binder-DNA complexes affecting the brightness of the bound dye.
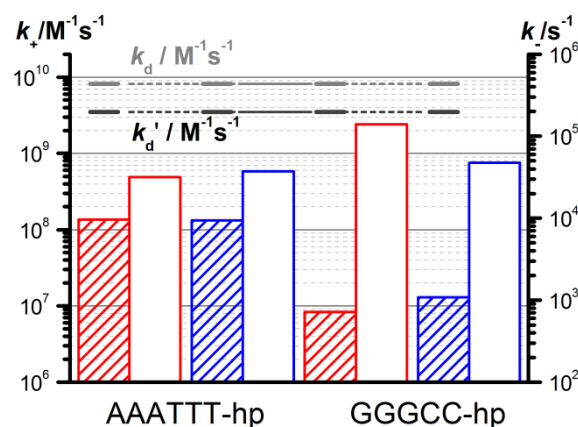
Figure 6. Association (filled bars, left scale) and dissociation (empty bars, right scale) rate constants of BBA-OG (red) and BBA-OG-long (blue) with DNA obtained from FCS. Estimates of the diffusion-controlled association rate contants k_d and k_d' for the formation of unlocalized (U) and localized (L) encounter complexes between binder and DNA (see reference [13]).

As previously reported,[13] BBA-OG shows much lower affinity constants to DNA than the parent BBA,[10] due to the high dissociation rate constants, that are several orders of magnitude higher than those of the typical minor-groove binders. For the AT sequence there is no change of the dissociation rate constant k_- due to the increase of the linker length in BBA-OG-long, but a 3-fold decrease of k_- is observed for the GC site (Table 5 and Figure 6). This result supports the hypothesis that repulsion between the negatively charged OG fluorophore and the DNA phosphate backbone is responsible for the high dissociation constants of these binders. In BBA-OG-long the longer linker between OG and BBA would reduce this electrostatic repulsion, especially when binding to the less specific GC DNA that also shows steric hindrance for the specific interactions between BBA and the minor groove, as discussed below.

Instead, the association rate constants are scarcely affected by lengthening the linker between BBA and OG (Table 5 and Figure 6). The values of k_+ are approximately an order of magnitude higher for the sequence AAATTT than for the GGCCC and mainly determine the specificity of the binders to AT sites. Nevertheless, specificity is significantly lower for BBA-OG-long in comparison to BBA-OG due to the decrease in k_- for the GC sequence.

The fact that the association rate constant, and very especially its relative values among the sequences, is barely affected by the length of the linker supports our premise that the association process for this type of binders is independent of the attachment of a label to the binder. The results obtained show that the association rate constants of DNA minor-groove binders are far below the diffusion-controlled limit, even if the lower diffusion-controlled association rate constant k_d' for the formation of a localized encounter complex (where the binder is located near the reactive sequence of DNA) is consider (see Figure 6 and reference [13]). This means that the rate-limiting step of the association process is not the formation of the encounter complex but the unimolecular inclusion of the binder into the minor groove of DNA, which is determined by sterical requirements. Therefore, there is room for an improvement of binder specificity by modifying the geometry and spatial orientation of the binder in order to fit better in the AT minor groove.

Furthermore, a positively charged dye instead of OG should be used in order to increase (or at least not to decrease) the affinity of BBA to DNA, since electrostatic repulsion would be avoided. Nevertheless, photophysical studies on the interactions between BBA and the dye should be performed for a best choice where the fluorescence enhancement upon binding is preserved.

Conclusion

Our studies on BBA-OG and BBA-OG-long have shown that very sensitive fluorogenic binders can be designed by linking a suitable dye to the desirable DNA binder. The detailed photophysical analysis allowed us to identify static and dynamic quenching by Photoinduced Electron Transfer (PET) between BBA and OG as the process responsible for the unusually strong change in brightness observed in BBA-OG. Free BBA-OG forms efficiently an intramolecular complex, both in the ground and in the excited state. In this sandwich-like conformation the fluorescence of OG is very efficiently quenched by PET to BBA.

The insertion of BBA into the minor groove of dsDNA hinders the formation of the complex and thus interrupts PET. This quenching interaction between the two moieties provides a direct way to create detectable fluorescence signals upon binding. Due to its strong distance dependence and high efficiency, PET is a very convenient photophysical mechanism to achieve a high brightness ratio between bound and free binder that, in addition, can be modulated by the linker length between the binding moiety and the fluorescent dye.

Dynamic studies of these binders by FCS yield precise values of the association and dissociation rate constants, which are not easily obtainable with other techniques. These results help us to understand the dynamics of the binding process, which in turn define the affinity and specificity of this type of binders.

The association rate constants are neither influenced by the attachment of OG to BBA nor by the increase of the linker length. The process of the association of these fluorogenic binders to dsDNA is therefore very similar to that of BBA alone and probably to that of other typical minor groove binders.

In contrast, the dissociation rate constants of BBA-OG and BBA-OG-long are much higher than those of typical minor-groove binders. The electrostatic repulsion between the negatively charged dye OG and the DNA weakens the stabilization of the BBA moiety within the minor groove. This effect can be reduced to some extent by increasing the linker length between BBA and OG. The lower affinity of BBA-OG and BBA-OG-long to dsDNA as compared to BBA alone is therefore mainly a consequence of their weaker attachment to the minor groove and the resulting faster dissociation.

The results obtained for the two binders also show that their specificity to different dsDNA sequences is mainly defined by the association process, which could be improved with a modified design of the binding moiety.

The detailed understanding of the photophysical and dynamic behavior of these prototypical binders will allow us to go one step further in the design of improved DNA binders with tunable fluorescence and binding properties.

Experimental Section

Materials

Oregon Green® 488 carboxylic acid (5-isomer) (**OG**) was purchased from Molecular Probes. At pH 7.5 OG is in its trianionic form (the highest pK_a is 4.8[26]) and no significant changes in pK_a were observed when this fluorophore is attached to BBA.

Oligonucleotides were purchased lyophilized from Thermo Fisher Scientific Inc. They were reconstituted in buffer (Tris HCl 20mM, NaCl 100mM, pH=7.5) and annealed by heating to 95ºC followed by slow cooling to room temperature. DNA concentration was determined from the absorbance at 260 nm, using a typical value for the DNA molar absorptivity (1 OD = 50 µg/ml for dsDNA).[38] The ratio between the absorbances at 260 nm and 280 nm was checked to always be between 1.7 and 1.8, as an indicator of purity. The oligonucleotides used in this work were hairpins of 12 base-pairs + loop with the following sequences (5' to 3'): AAATTT-hp (GGC **AAATTT** CGC TTTTT GCG **AAATTT** GCC) and GGCCC-hp (GGCA **GGCCC** AGC TTTTT GCT **GGGCC** TGCC).

Synthesis and purification

The synthesis and purification of the bis-amino-benzamidine BBA in Figure 1 (4-{[(3-{[(4-carbamimidoylphenyl)amino]methyl}-5-(aminopropoxy)propane)phenyl]

methyl]amino}-benzene-1-carboximidamide), which was used in the preparation of BBA-OG and for the photophysical studies, was achieved following previously published procedures.[13] The synthesis and purification of 5-{[3-({5-[3,5-bis({[(4-carbamimidoylphenyl)amino]methyl}) phenoxy]pentyl}-oxy)propyl]carbamoyl}-2-(2,7-difluoro-6-hydroxy-3-oxo-3H-xanthen-9-yl)benzoic acid (BBA-OG-long) is described in detail in the SI.

Sample Preparation

All samples were prepared in buffer (Tris HCl 20mM, NaCl 100mM, pH=7.5). Stock solutions of the dyes and of the different DNAs were freshly prepared for each series. Dye concentration of the samples was $2 – 5 \times 10^{-7}$ mol dm^{-3} for conventional fluorescence measurements and about 100 times lower for FCS measurements. The samples for FCS titrations were prepared by the dilution-extraction method beginning with a concentrated DNA solution containing the desired concentration of the binder and diluting with a solution of the binder of the same concentration.

Equipment and techniques

Absorption spectra were recorded using quartz cells with an absorption path length of 10.0 mm in a Varian-Cary 100 spectrometer. Steady-state and time-resolved fluorescence measurements were performed with an Edinburgh-Instruments F900 spectrofluorimeter, equipped with a Xenon lamp of 450 W as excitation source for fluorescence spectra and a diode laser EPL-470 nm for fluorescence lifetime measurements. All experiments were carried out at 25 ± 1 ºC.

The home built FCS apparatus has been described elsewhere.[36] The specific setup used for the FCS measurements presented in this study is given in detail in the SI. The samples were excited by the continuous light of a 489 nm laser diode. Fluorescence was discriminated from scattered laser light with band-pass filters centered at 525 nm (45 nm bandwidth) and detected by two avalanche photodiodes. Typically 20 million photons were collected for each correlation curve. The focal area and the detection volume were calibrated with Rhodamine 123 in aqueous solution with low irradiance yielding a radial $1/e^2$ radius of $w_{xy} = 0.53$ µm. The value of $D_{R123}(25ºC)= (4.6 \pm 0.4) \times 10^{-10}$ m^{2}s^{-1} is estimated from PFG-NMR[39] and dual-focus FCS[40] data. The diffusion coefficients are given for 25°C.

Data Analysis

The series of absorption and emission spectra were analyzed using a program developed in our group that applies Principal Components Global Analysis (PCGA).[41, 42] The first step of PCGA is the Principal Components Analysis (PCA), which yields the minimal number of components that reproduce the experimental spectra, i.e. it allows one to determine the minimum number of chemical species that contribute to the spectra. This step helps to propose a mechanism that explains the observed variations necessary in the second step, the Global Analysis (GA). GA consists in the fit of the theoretical model to the whole series of experimental spectra to estimate the model parameters and the pure spectra of the contributing species.

Individual fits of fluorescence decays were performed with the software package from Edinburgh Instruments. The series of fluorescence decays measured at different surfactant concentrations together with the corresponding pulse responses were also fitted globally using a home-made program in Matlab (The MathWorks, US).

A FCS correlation curve is the normalized autocorrelation function $G(\tau)$ of the fluorescence intensity fluctuations that represents the probability to register from the same molecule a second photon at the correlation time τ, once a first photon was emitted and is calculated as follows:

$$G(\tau) = \frac{\langle \delta F(t) \cdot \delta F(t+\tau) \rangle}{\langle F(t) \rangle^2} \tag{4}$$

FCS curves were fitted using a dynamic-equilibrium model that has been described in previous articles.[14-17] Two levels of nonlinear data analysis were applied: i) individual fit of each correlation curve to the function $G(\tau)$ given in

equation (5) that is composed by a diffusion term (G_D) and two bunching terms corresponding to the triplet formation (G_T) and the binding reaction (G_R), and ii) global fit of a series of correlation curves obtained by titration of the binders with DNA to equation (5) with the concentration-dependent parameters modelled as function of DNA concentration, as given in equations (6) - (8), using a home-made global "target" analysis program in Matlab (The MathWorks, US). An empirical weighting function was used in order to take into account the strong variation of the noise in the FCS curves.

$$G(\tau) = G_D \cdot G_T \cdot G_R$$

$$G(\tau) = \frac{1}{N}\left(1+\frac{\tau}{\overline{\tau}_D}\right)^{-1}\left(1+\left(\frac{w_{xy}}{w_z}\right)^2\frac{\tau}{\overline{\tau}_D}\right)^{-\frac{1}{2}} \cdot \left(1 + A_T \, e^{-\tau/\tau_T}\right) \cdot \left(1 + A_R \, e^{-\tau/\tau_R}\right) \tag{5}$$

$$\overline{\tau}_D = \frac{\tau_f(1+K[DNA]_0)}{1+\frac{\tau_f}{\tau_b}K[DNA]_0} \tag{6}$$

$$\tau_R = (k_+[DNA]_0 + k_-)^{-1} = (k_-(1+K[DNA]_0))^{-1} \tag{7}$$

$$A_R = \frac{K[DNA]_0(1-q)^2}{(1+qK[DNA]_0)^2} \tag{8}$$

In these equations $\overline{\tau}_D$ is the mean diffusion time, which can be expressed as a function of the diffusion correlation times of free (τ_f) and bound dye (τ_b) and the binding equilibrium constant K; τ_R is the reaction relaxation time, which depends on the association (k_+) and the dissociation (k_-) rate constants that are related to the equilibrium constant by the equation $K = k_+/k_-$; and A_R is the amplitude of the reaction term which is a function of K and of the brightness ratio q between bound and free dye. In the first term of equation (5) N is the mean number of fluorescent molecules within the detection volume. The second term is due to triplet formation with a correlation time that corresponds to the triplet lifetime of the dye τ_T and the amplitude A_T that is related to the fraction of excited molecules going into the "dark" triplet state. This amplitude increases with the irradiance applied to the sample so that the triplet term can be distinguished from the reaction term by measuring FCS curves at increasing irradiances (power series).

FCS curves may show baseline distortions due to residual slow intensity fluctuations that must be corrected by adding an additive fit parameter b to equation (5). Moreover, the presence of impurities and scattering can have an influence on different parameters of the FCS curve. Thus, the mean number of particles in the sample volume N is strongly affected by scattering and weakly fluorescent impurities of DNA.[43] Otherwise, small amounts (<1%) of highly fluorescent free dye OG remaining after purification of the binders, especially in the case of BBA-OG-long, cause a perceptible decrease of the observed diffusion correlation time of the binders. This effect is taken into account by a suitable correction in the diffusion term of equation (5).[43]

Note that the symbol τ is usually used to denote fluorescence lifetimes but also for the correlation time. In this work it is used for both properties but the subscripts allow discerning among the different lifetimes and correlation times involved.

Unless otherwise indicated, all given uncertainties are the standard deviations estimated in the fits and do not take into account the accuracy of the DNA concentrations.

[1] M. J. Waring, *Sequence-specific DNA binding agents*, Royal Society of Chemistry **2006**.

[2] S. Neidle in Principles of Nucleic Acid StructureAnonymous , Academic Press, New York, **2008**, pp. 132-203.

[3] E. Pazos, J. Mosquera, M. E. Vázquez, J. L. Mascareñas, *ChemBioChem* **2011**, *12*, 1958-1973.

[4] V. C. Rucker, A. R. Dunn, S. Sharma, P. B. Dervan, H. B. Gray, *J. Phys. Chem. B* **2004**, *108*, 7490-7494.

[5] V. C. Rucker, S. Foister, C. Melander, P. B. Dervan, *J. Am. Chem. Soc.* **2003**, *125*, 1195-1202.

[6] E. J. Fechter, B. Olenyuk, P. B. Dervan, *J. Am. Chem. Soc.* **2005**, *127*, 16685-16691.

[7] O. Vázquez, M. I. Sánchez, J. Martínez-Costas, M. E. Vázquez, J. L. Mascareñas, *Org. Lett.* **2010**, *12*, 216-219.

[8] O. Vázquez, M. I. Sánchez, J. L. Mascareñas, M. E. Vázquez, *Chem. Commun.* **2010**, *46*, 5518-5520.

[9] M. I. Sánchez, O. Vázquez, M. E. Vázquez, J. L. Mascareñas, *Chem. Commun.* **2011**, *47*, 11107-11109.

[10] M. I. Sánchez, O. Vázquez, J. Martínez-Costas, M. E. Vázquez, J. L. Mascareñas, *Chem. Sci.* **2012**, *3*, 2383-2387.

[11] M. I. Sánchez, O. Vázquez, M. E. Vázquez, J. L. Mascareñas, *Chem. Eur. J.* **2013**,.

[12] M. I. Sánchez, C. Penas, M. E. Vázquez, J. L. Mascareñas, *Chemical Science* **2014**, *5*, 1901-1907.

[13] J. Bordello, M. I. Sánchez, M. E. Vázquez, J. L. Mascareñas, W. Al-Soufi, M. Novo, *Angew. Chem. Int. Ed.* **2012**, *51*, 7541-7544.

[14] W. Al-Soufi, B. Reija, M. Novo, S. Felekyan, R. Kühnemuth, C. A. M. Seidel, *J. Am. Chem. Soc.* **2005**, *127*, 8775-8784.

[15] M. Novo, S. Felekyan, C. A. M. Seidel, W. Al-Soufi, *J. Phys. Chem. B* **2007**, *111*, 3614-3624.

[16] W. Al-Soufi, B. Reija, S. Felekyan, C. A. Seidel, M. Novo, *ChemPhysChem* **2008**, *9*, 1819-1827.

[17] J. Bordello, M. Novo, W. Al-Soufi, *J. Colloid Interface Sci.* **2010**, *345*, 369-376.

[18] A. van Oijen, *Curr. Opin. Biotechnol.* **2011**, *22*, 75-80.

[19] C. K. Nandi, P. P. Parui, T. L. Schmidt, A. Heckel, B. Brutschy, *Anal. Bioanal. Chem.* **2008**, *390*, 1595-1603.

[20] M. Ritzefeld, V. Walhorn, C. Kleineberg, A. Bieker, K. Kock, C. Herrmann, D. Anselmetti, N. Sewald, *Biochemistry* **2013**, *52*, 8177-8186.

[21] K. S. Grußmayer, T. Ehrhard, K. Lymperopoulos, D. Herten, *Biophys. Chem.* **2013**, *184*, 1-7.

[22] R. Baliga, D. M. Crothers, *J. Am. Chem. Soc.* **2000**, *122*, 11751-11752.

[23] R. Baliga, D. M. Crothers, *Proc. Natl. Acad. Sci.* **2000**, *97*, 7814-7818.

[24] S. Y. Breusegem, S. Sadat-Ebrahimi, K. T. Douglas, R. M. Clegg, F. G. Loontiens, *J. Mol. Biol.* **2001**, *308*, 649-663.

[25] S. Y. Breusegem, R. M. Clegg, F. G. Loontiens, *J. Mol. Biol.* **2002**, *315*, 1049-1061.

[26] W. Sun, K. R. Gee, D. H. Klaubert, R. P. Haugland, *J. Org. Chem.* **1997**, *62*, 6469-6475.

[27] D. Magde, R. Wong, P. G. Seybold, *Photochem. Photobiol.* **2002**, *75*, 327-334.

[28] K. Tanaka, T. Miura, N. Umezawa, Y. Urano, K. Kikuchi, T. Higuchi, T. Nagano, *J. Am. Chem. Soc.* **2001**, *123*, 2530-2536.

[29] T. Miura, Y. Urano, K. Tanaka, T. Nagano, K. Ohkubo, S. Fukuzumi, *J. Am. Chem. Soc.* **2003**, *125*, 8666-8671.

[30] T. Hirano, K. Kikuchi, Y. Urano, T. Nagano, *J. Am. Chem. Soc.* **2002**, *124*, 6555-6562.

[31] H. Zhang, M. Zhang, T. Shen, *J. Photochem. Photobiol. A.* **1997**, *103*, 63-67.

[32] J. R. Lakowicz, *Principles of Fluorescence Spectroscopy*, Springer, USA, **2006**.

[33] C. A. Seidel, A. Schulz, M. H. Sauer, *J. Phys. Chem.* **1996**, *100*, 5541-5553.

[34] S. Freire, J. Bordello, D. Granadero, W. Al Soufi, M. Novo, *Photochem. Photobiol. Sci.* **2010**, *9*, 687-696.

[35] D. Matulis, R. Lovrien, *Biophys. J.* **1998**, *74*, 422-429.

[36] D. Granadero, J. Bordello, M. J. Pérez-Alvite, M. Novo, W. Al-Soufi, *Int. J. Mol. Sci.* **2010**, *11*, 173-188.

[37] M. M. Tirado, C. L. Martínez, J. G. de la Torre, *J. Chem. Phys.* **1984**, *81*, 2047.

[38] G. Kallansrud, B. Ward, *Anal. Biochem.* **1996**, *236*, 134-138.

[39] P. O. Gendron, F. Avaltroni, K. J. Wilkinson, *J. Fluoresc.* **2008**, *18*, 1093-1101.

[40] C. Muller, A. Loman, V. Pacheco, F. Koberling, D. Willbold, W. Richtering, *Europhys. Lett.* **2008**, *83*, 46001.

[41] W. Al-Soufi, M. Novo, M. Mosquera, *Appl. Spectrosc.* **2001**, *55*, 630-636.

[42] W. Al-Soufi, M. Novo, M. Mosquera, F. Rodríguez-Prieto, *Reviews in Fluorescence 2009* **2011**, 23-45.

[43] J. Bordello Malde, *PhD Thesis, University of Santiago de Compostela,* **2013**.

Entry for the Table of Contents (Please choose one layout only)

Layout 2:

FULL PAPER
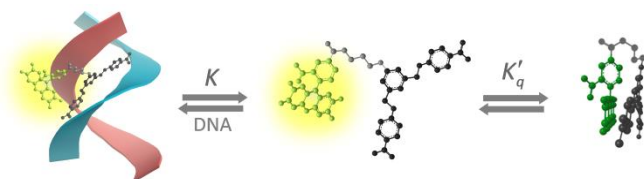
The detailed photophysical study of fluorogenic binders obtained by labeling a bisbenzamidine with the dye Oregon Green shows that quenching by Photoinduced Electron Transfer (PET) is responsible for their huge fluorescence enhancement upon binding to the minor groove of dsDNA. Fluorescence Correlation Spectroscopy (FCS) yields precise association and dissociation rate constants that help to understand and optimize the specificity and affinity of these binders to DNA.

█ Subject Heading

Jorge Bordello[, Mateo I. Sánchez, M. Eugenio Vázquez, José L. Mascareñas, Wajih Al-Soufi and Mercedes Novo*

██ – ██

Fluorescence-labelled Bis-benzamidines as Fluorogenic DNA Minor-Groove Binders: Photophysics and Binding Dynamics